

Evaluation of Green's Function Integrals in Conducting Media

Swagato Chakraborty* and Vikram Jandhyala

Department of Electrical Engineering, University of Washington, Seattle WA 98195
Phone: 206-543-2186, Fax: 206-543-3842, Email: jandhyala@ee.washington.edu

1. Introduction

Method of moments (MoM) solvers are useful for simulating coupled circuit-electromagnetic problems [1] involving integrated circuit packages and systems-on-chip, wherein frequency-dependent skin effects can be modeled, and arbitrarily-shaped structures such as on-chip inductors can be analyzed with surface-only formulations. For broadband analog and digital applications, spectral current and field components can arise at sufficiently low frequencies where surface impedance approximations [2] for approximating skin effects are not valid. For seamless surface-based broadband simulation, it is important to explicitly model the interior of conducting materials in order to avoid ad-hoc mixing of surface and volume based formulations. This paper focuses on broadband computation of lossy medium scalar, vector, and gradient Green's function integrals for arbitrarily located sources and observers.

Existing methods for computing Green's function integrals address subsets of the above problem; for instance, singularity extraction [3] in conjunction with 2D Gaussian quadrature [4] can be used for computation of Green's function integrals in lossy media at very low frequencies where exponential spatial decays are weak. Methods suitable for computing Green's function integrals at high frequencies are discussed previously in [5] for lossless media and in [6] for lossy media, for the restricted case of the scalar Green's function. A similar approach is proposed in [7] to evaluate the scalar and the vector cases for self-term integration, with extensions possible in-plane observation. However, the crucial case of near-singular observation points outside the plane, as in the modeling of very thin conductors cannot be handled by the approach in [7]. The computation of gradient Green's function integrals has not been addressed by the methods [5-7].

In this work we propose a polar-coordinate transformation and new mixed analytic and numerical quadrature for accurate evaluation of RWG function [8] based scalar, vector, and gradient Green's function integrals in lossy conducting media in a form more general than other existing methods. The presented technique is broadband and applicable to any distribution of source and testing function locations and orientations and to any lossy material.

2. Formulation and Resultant Integrals

The magnetic and electric potentials due to an RWG basis function in a lossy medium can be described as linear combinations of four two-dimensional integrals M_{vect} [7], M_{scal} [5-6], N_{vect} and N_{scal} [9] given as

$$M_{\text{vect}} = \iint_T \boldsymbol{\rho} \frac{e^{-jkR}}{R} ds', \quad M_{\text{scal}} = \iint_T \frac{e^{-jkR}}{R} ds' \quad (2.1a)$$

$$N_{\text{vect}} = \iint_T \boldsymbol{\rho} \frac{e^{-jkR}(1+jkR)}{R^3} ds', \quad N_{\text{scal}} = \iint_T \frac{e^{-jkR}(1+jkR)}{R^3} ds' \quad (2.1b)$$

where T denotes a source triangle, $\boldsymbol{\rho}$ is the vector from the projection O of the observation point \mathbf{r} on the plane of T to a source point \mathbf{r}' in T , and $R = |\mathbf{r} - \mathbf{r}'|$ is the

radial distance between the source and the observation point. R can be written as $R = \sqrt{\rho^2 + d^2}$, where d denotes the distance of the observation point \mathbf{r} from the plane of T . The complex wave-number in the interior of the conductor is denoted by k . Equation (2.1a) can be expressed in polar coordinates as

$$\mathbf{M}_{\text{vect}} = \hat{\mathbf{x}} \int_{\rho_{\min}}^{\rho_{\max}} \frac{\rho^2 e^{-jk\sqrt{\rho^2+d^2}}}{\sqrt{\rho^2+d^2}} \left(\int_{\theta_{\min}(\rho)}^{\theta_{\max}(\rho)} \cos\theta d\theta \right) d\rho + \hat{\mathbf{y}} \int_{\rho_{\min}}^{\rho_{\max}} \frac{\rho^2 e^{-jk\sqrt{\rho^2+d^2}}}{\sqrt{\rho^2+d^2}} \left(\int_{\theta_{\min}(\rho)}^{\theta_{\max}(\rho)} \sin\theta d\theta \right) d\rho \quad (2.2)$$

where local two-dimensional x-y coordinates have been used in the plane of T and θ is the polar angle of a source point \mathbf{r}' relative to the local coordinate system with origin at O . The limits on ρ are given by its extremals for which a circle with radius ρ centered at O intersects T . The limits on θ for a given ρ are obtained by finding the intersection points of T with the circle of radius ρ . In general, the four integrals in Eqns. (2.1a,b) can be recast into polar coordinates to obtain separable integrals of the form

$$I = \int_{\rho_{\min}}^{\rho_{\max}} f(\rho, k, d) \left(\int_{\theta_{\min}(\rho)}^{\theta_{\max}(\rho)} g(\theta) d\theta \right) d\rho \quad (2.3)$$

The integral in Eqn. (2.3) is separable in its variables ρ and θ , and the integral in θ has a simple closed form expression. Thus the overall integral can finally be expressed as a

$$1\text{D integral in } \rho \text{ as, } I = \int_{\rho_{\min}}^{\rho_{\max}} u(\rho) d\rho.$$

It is important to note the change in order of integration compared to that in [5-7], where the (analytic) integration is done first on ρ . While [5-6] consider only the scalar integral, in [7] the on-plane observer locations ($d = 0$) lead to functions of ρ for the vector integral that are easily integrable, which is not the case for general observation points ($d \neq 0$). To obviate this problem, particularly for the crucial case of near singular off-plane observation points, the change in order of integration is performed in our work. In the proposed method, $g(\theta)$ is always a simple sinusoidal function or a constant, due to the fact that the Green's functions are not dependent on the polar angle θ . Therefore the θ integral can be computed analytically in all cases (arbitrary locations, materials, frequencies, and scalar, vector, and gradient integrals), leading to a final 1D numerical integration in ρ , of the integrand $u(\rho)$, which is a continuous and piece-wise smooth function in the interval $(\rho_{\min}, \rho_{\max})$. Boundaries of the subintervals of ρ over which $u(\rho)$ is smooth, are the radii values for which the circle touches the vertices of T or its edges tangentially. An adaptive 1D integration rule has been developed for the functions above using an approach similar to Matlab's *quad8*.

3. Numerical Results

A relative accuracy comparison between the proposed scheme and fixed-point two-dimensional Gaussian quadrature with singularity extraction is demonstrated in Fig. 1 for the interior of a Copper conductor. At low frequencies, the Green's functions in lossy media exhibit slow decay over distance and hence a 7-point Gaussian quadrature scheme [4] functions adequately. As the frequency is increased, the details of the sharp exponential decay in the Green's functions are not captured by the low-order Gaussian rule. The presented formulation explicitly models the exponential decays and is thus not affected by the added detail. To confirm that the 7-point Gaussian rule has broken down for this case, a higher-order 25-point Gaussian quadrature scheme is also used. This

method shows better accuracy than the lower order rule in the range of 100-1000 Hz. However, as is evident, as the frequency is increased further, the 25-point rule also becomes inaccurate. In general, any fixed-order two-dimensional rule will become inaccurate after a certain frequency. While this has not been explicitly verified in this paper, it is expected that a well-designed 1D adaptive quadrature scheme should outperform an adaptive two-dimensional quadrature rule for the reasons that the exponential decay is explicitly extracted in the 1D form, making amenable the use of a specialized quadrature rule (e.g. Gauss-Laguerre [4]), and that the explicit independence of the Green's function on the polar angle is exploited in the 1D form.

Figure 2 demonstrates the ability of the proposed method in conjunction with a coupled two-region circuit-EM MoM formulation [1] to compute the frequency-dependent resistance of a cylinder, with radius 0.5 mm. and length 5 mm, including the low-frequency leveling off behavior to the DC value of 0.109Ω , using a two-region PMCHW formulation [10]. Also shown is the solution from the surface impedance approximation, which becomes inaccurate at low frequencies (Fig.2, left) but provides the correct answer at higher frequencies (Fig.2, right). A fixed-point two-dimensional Gaussian rule gives correct answers at very low frequencies (Fig.2, left) but is inaccurate above a certain frequency (Fig.2, right).

4. Conclusions

In this paper, a new approach to evaluate the Green's function operators for RWG functions in conducting media is presented. The method works for arbitrarily located sources and observers for any frequency. This technique has been incorporated into a broadband two-region surface formulation for accurate computation of frequency-dependent parameters, and shows the potential to obviate the need to switch to volumetric formulations at low frequencies where skin effect is not well developed.

Acknowledgements

This work was partially supported by DARPA-MTO NeoCAD grant N66001-01-1-8920, NSF-CAREER grant ECS-0093102, NSF-SRC Mixed-Signal Initiative grant CCR-0120371, and by a grant from Ansoft Corporation.

References

- [1] V. Jandhyala, W.Yong, D.Gope, and R. Shi, "Coupled electromagnetic-circuit simulation of arbitrarily-shaped conducting structures using triangular meshes," *Proceedings International Symposium on Quality Electronic Design*, pp. 38-42, Mar. 2002.
- [2] A.W.Glisson, "Electromagnetic scattering by arbitrarily shaped surfaces with impedance boundary conditions," *Radio Science*, vol. 27(6), pp. 935-943, Nov. 1992.
- [3] R.D. Graglia, "On the numerical integration of the linear shape function times the 3-D Green's function or its gradient on a planar triangle," *IEEE Transactions on Antennas and Propagation*, vol. 41, pp. 1448-1455, 1993.
- [4] M. Abramowitz and I. Stegun, Chapter 25, *Handbook of Mathematical Functions*, Dover, New York, 1970.
- [5] M. Gimersky, S. Amari, and J. Bornemann, "Numerical evaluation of the two-dimensional generalized exponential integral," *IEEE Transactions on Antennas and Propagation*, vol. 44, pp. 1422-1425, 1996.
- [6] Z. Zhu, J. Huang, B. Song, and J. White, "Improving the robustness of a surface integral formulation for wideband impedance extraction of 3D structures," *Proceedings of International Conference on Computer Aided Design*, pp. 592-597, 2001.
- [7] L. Rossi and P.J. Cullen, "On the fully numerical evaluation of the linear-shape function times the 3-D Green's function on a planar triangle," *IEEE Transactions on Microwave Theory and Techniques*, vol. 47, pp. 398-402, 1999.

- [8] S.M. Rao, D.R.Wilton, and A.W. Glisson, "Electromagnetic scattering by surfaces of arbitrary shape," *IEEE Transactions on Antennas Propagation*, vol. 30, pp. 409-418, 1982.
- [9] R.E.Hodges and Y.Rahmat Samii, "The evaluation of MFIE integrals with the use of vector triangle basis function," *Microwave and Optical Technology Letters*, vol. 14 (1), pp. 9-14, Jan.1997.
- [10] K.Umashankar, A.Taflove, and S.M.Rao, "Electromagnetic scattering by arbitrary shaped three dimensional homogeneous lossy dielectric objects," *IEEE Transactions on Antennas and Propagation*, Vol 34(6), pp. 758-766, June 1986.

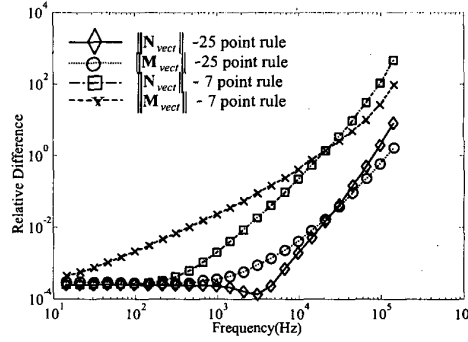


Figure 1: Comparison between 2D Gaussian rules with singularity extraction and proposed method for evaluation of the integrals M_{vecr} and N_{vecr} in Eqns. (2.1a,b) for a non-self-term integral, for a triangle with vertices $(\alpha, -\alpha, 0), (\alpha, \alpha/2, 0), (-2\alpha, \alpha/2, 0)$, and observation point located at $(0, 0, \alpha)$, where $\alpha = 1 \text{ mm}$, with $\sigma = 5.8 \times 10^7 \text{ S/m}$.

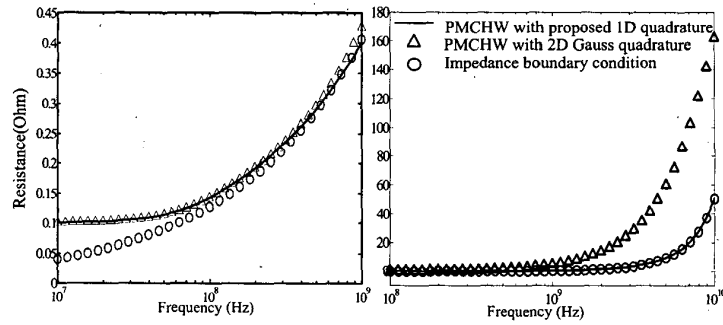


Figure 2: Extracted resistance of a cylinder of radius 0.5mm and length 5 mm with $\sigma = 5.8 \times 10^4 \text{ S/m}$ using a two region PMCHW formulation with the standard 7-point 2D Gaussian quadrature method and the method proposed in this paper, and an impedance boundary condition formulation, for a low frequency band (left) and higher frequencies (right).